Geological Survey of Canada

CURRENT RESEARCH
2005-D2

Field and laboratory measurements of magnetic properties and density, Central Metasedimentary Belt, Ontario

Clare O'Dowd and David Eaton

2005

CURRENT RESEARCH

Natural Resources Canada Ressources naturelles Canada

Canada

ISSN 1701-4387
Catalogue No. M44-2005/D2E-PDF
ISBN 0-662-39645-6

A copy of this publication is also available for reference by depository libraries across Canada through access to the Depository Services Program's website at http://dsp-psd.pwgsc.gc.ca

A free digital download of this publication is available from the Geological Survey of Canada Bookstore web site:

http://gsc.nrcan.gc.ca/bookstore/

Click on “Free Download”.

Toll-free (Canada and U.S.A.): 1-888-252-4301

Authors’ address

D. Eaton (deaton@uwo.ca)
C. O’Dowd (codowd2@uwo.ca)
University of Western Ontario
London, Ontario N6A 5B7

Publication approved by GSC Pacific

Original manuscript submitted: 2004-10-14

Final version approved for publication: 2004-02-17

Field and laboratory measurements of magnetic properties and density, Central Metasedimentary Belt, Ontario

Clare O'Dowd and David Eaton

O'Dowd, C. and Eaton, D., 2005: Field and laboratory measurements of magnetic properties and density, Central Metasedimentary Belt, Ontario; Geological Survey of Canada, Current Research 2005-D2. 12 p.

Abstract: In situ magnetic susceptibility (*K*) and coincident ground magnetometer readings were measured at 26 locations within the Grenville Province near Bobcaygeon, Ontario. Hand samples were also collected for laboratory measurements of *K*, Königsberger ratio (*Q*) and density (ρ). Laboratory *K* measurements tended to be slightly greater than in situ measurements and are regarded here as more reliable; in situ measurements, however, provide useful information about the spatial distribution of *K* and its relationship to magnetic anomalies at various scales. Mafic gneisses yielded the highest average *K* (0.0125 SI) and ρ (2.914 Mg/m^3). Ordovician limestones yielded the lowest *K* (1.05´10^{-6} SI), but a surprisingly high average ρ (2.839 Mg/m^3). There is a good correlation of *K* and ρ with regional-scale anomalies, but at the outcrop scale the correlation of *K* with magnetic anomalies is not as clear.

Résumé : Des mesures in situ de la susceptibilité magnétique (*K*) et des mesures coïncidentes au magnétomètre de terrain ont été exécutées à 26 endroits dans la Province de Grenville près de Bobcaygeon (Ontario). Des échantillons ont en outre été prélevés à la main pour les soumettre à des mesures en laboratoire de *K*, du rapport de Königsberger (*Q*) et de la densité (ρ). En général, les mesures de K en laboratoire ont donné des résultats légèrement plus élevés que les mesures effectuées in situ et sont considérées plus fiables; les mesures in situ fournissent cependant des informations utiles quant à la répartition spatiale de *K* et B sa relation avec les anomalies magnétiques à diverses échelles. Des gneiss mafiques ont fourni les valeurs moyennes les plus élevées pour *K* (0,0125 SI) et pour ρ (2,914 Mg/m^3). Des calcaires ordoviciens ont donné les plus faibles valeurs de *K* (1,05 x 10^{-6} SI), mais une valeur moyenne de ρ (2,839 Mg/m^3) étonnamment élevée. Il existe une bonne corrélation entre les valeurs de *K* et ρ et les anomalies d'échelle régionale, mais la corrélation entre *K* et les anomalies magnétiques est moins évidente à l'échelle de l'affleurement.

INTRODUCTION

The Grenville Province, the youngest part of the Canadian Shield, is a northeast-trending belt that records regional metamorphism and plutonic activity associated with terrane accretion and inferred continent-continent collision ca.1200 to 980 Ma (Rivers, 1997). Within Ontario (Fig. 1), the Grenville Province occupies an area of north and west of the Phanerozoic cover, and south of the Grenville Front, roughly from Killarney to Lake Timiskaming. Grenvillian crust extends beneath up to 1 km of Paleozoic rocks in southern Ontario and continues in the subsurface beneath the midwestern United States. This study focuses on the Central Metasedimentary Belt and the Central Metasedimentary Belt boundary tectonic zone, an approximately 40 km wide tectonic belt that records ca.1080 to 1060 Ma northwestward ductile thrusting of the Central Metasedimentary Belt over the Central Gneiss Belt, part of the pre-Grenvillian Laurentian margin (Hanmer and MacEachern, 1992).

Magnetic and gravity anomaly maps play an important role in the interpretation of Grenvillian tectonic domains, particularly beneath the Paleozoic cover and the Great Lakes (Easton and Carter, 1995; Forsyth et al., 1994). For example, Ouassa and Forsyth (2002) identified magnetic fabrics beneath Paleozoic cover south of Lake Ontario (43°N, 78°W) that can be correlated with the Frontenac terrane of the Central Metasedimentary Belt. In the vicinity of the Paleozoic zero edge, the boundary tectonic zone is characterized by a negative total-field magnetic anomaly outlining linear to sinuous magnetic anomalies extending beneath western Lake Ontario and eastern Lake Erie (Milkereit et al., 1992) (Fig. 1). The boundary tectonic zone in this area has an associated Bouguer gravity low. To the east, the Central Metasedimentary Belt contains conspicuous curvilinear positive anomalies with a north-northeast to northeast strike, as well as subcircular and annular positive anomalies associated with plutonic intrusions (Ouassa and Forsyth, 2002). The Central Gneiss Belt is characterized by subdued magnetic anomalies of indistinct shape, as well as subordinate northeast-striking

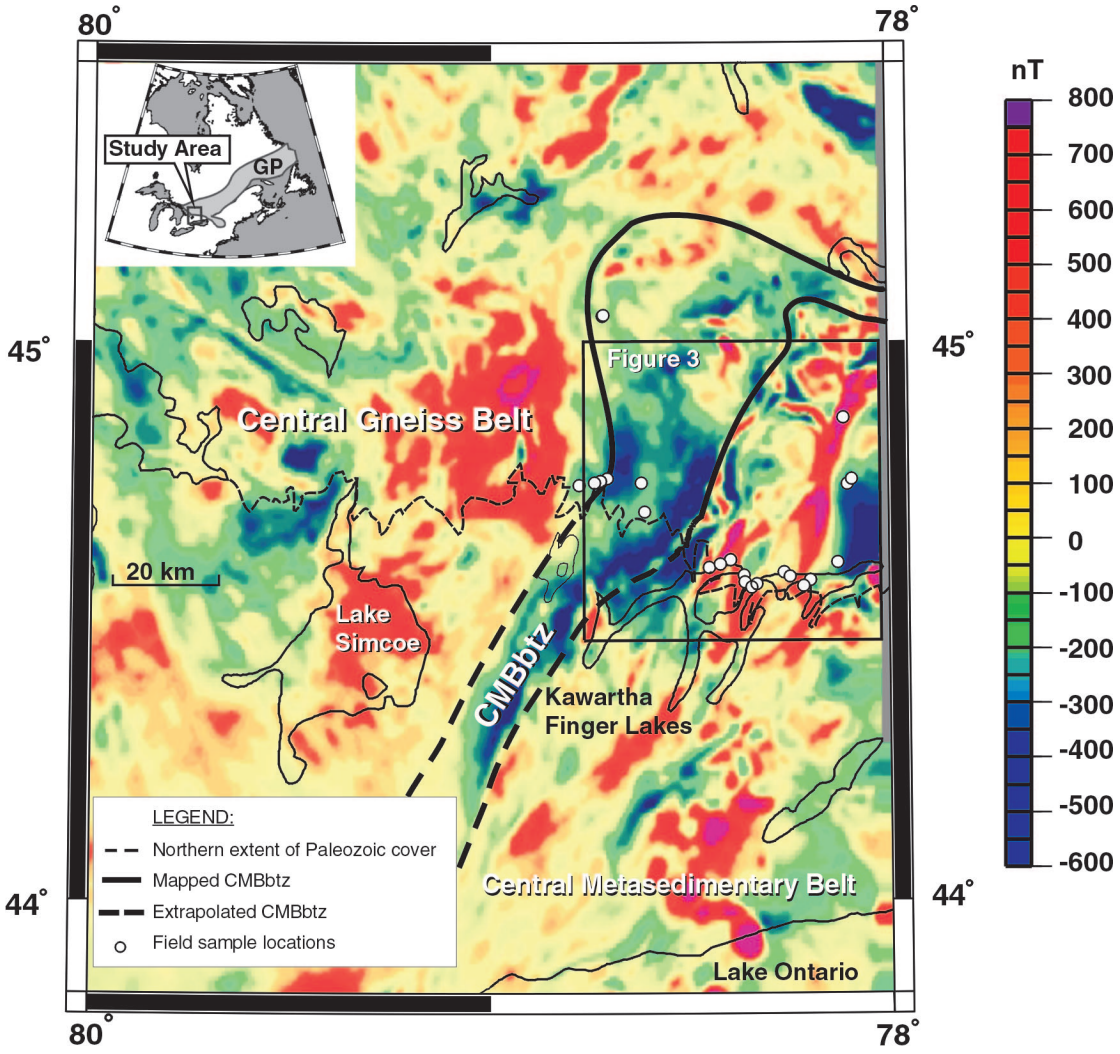

Figure 1. *Total-field aeromagnetic anomaly map of south-central Ontario. Tectonic boundaries are modified from Easton and Carter (1995). GP – Grenville Province, CMBbtz – Central Metasedimentary Belt boundary tectonic zone.*

Table 1. Technical specifications of field instruments.

GMS-2 Magnetic-susceptibility meter	
Sensitivity	1 x 10^{-5} K SI
Resolution	1 x 10^{-5} K SI
Signal Frequency	760 Hz
Sampling Rate	10 Hz
G-846 Portable proton magnetometer	
Resolution	Ten nT without staff
Tuning range	20 000 to 100 000 nT (worldwide)
Gradient tolerance	2 000 nT per metre
Sample rate	Five digit, illuminated display directly in nT

Table 2. Technical specifications of laboratory instruments.

SI2B Magnetic-susceptibility meter	
Sensitivity	Volume dependent; for 11 cm^3 sample stdev = 2 x 10^{-7}
Operating frequency	<13, 800 Hz
Coil	160 cm^3 volume internal coil
Range	2 x 10^{-7} <<3 SI
Precision	2 digits for 1 x 0^{-5} SI and 6 digits for 2.5 SI
Schonstedt Instrument Company digital spinner magnetometer	
Rotation rate	5 Hz
Resolution	No less than 1 mA/m

linear anomalies. The regional Bouguer gravity field in this region is smooth, with contours roughly parallel to the trend of the boundary tectonic zone (Lidiak and Hinze, 1993).

Although useful qualitative interpretations of magnetic and gravity maps are possible based on fabric analysis and geometrical relationships between inferred domains, more quantitative studies such as inversion require physical rock-property data. This study documents the magnetic properties and densities of exposed units in the Central Metasedimentary Belt, Central Metasedimentary Belt boundary tectonic zone, and part of the Central Gneiss Belt, which are situated between the Kawartha Finger Lakes and the Bancroft region (Fig. 1). Closely spaced in situ magnetic-susceptibility measurements are complemented here by laboratory measurements, which provide more controlled conditions but sparser sampling. Through examination of the exposed rocks and determination of their physical characteristics, magnetic and gravity interpretations can be tested and better constrained. Details of the equipment used are provided in Tables 1 and 2.

FIELD METHODS

Sampling locations

The goal of the sampling program was to identify and collect a representative suite of samples from the primary lithological units of both the Central Metasedimentary Belt and Central Metasedimentary Belt boundary tectonic zone, as outlined in Table 3, in order to record spatial variability of magnetic properties and density. The primary sampling corridor was located along Highway 36 (~44.6°N) to Highway 28(~57.15°W). This corridor, approximately centred near the town of Bobcaygeon, was selected because it transects several prominent regional magnetic anomalies. Additional sites to the north of Bancroft, along highways 62 and 35 just north of Minden, were chosen because of their association with other prominent magnetic anomalies. Sampling locations were scouted on July 6th, 2003; samples were collected and in situ measurements made July 14 to 17th, 2003.

While general locations were determined using regional gravity and magnetic maps, specific sampling sites were chosen in the field. The area covered by the sample population is large, and so all sampling was completed along roadcuts. Stations were selected on the basis of exposure, lithology, accessibility, and safety.

Sampling methodology

To allow for testing of scaling behaviour, statistical variability, and anisotropy, several different sampling methodologies were attempted. Figure 2 illustrates typical outcrop sampling locations and methodology.

Importance was placed on sampling of magnetic-susceptibility readings so that the spatial statistics of the data set are well represented, to aid in extrapolation to areas where data are lacking. At a few stations a pseudo-random sampling methodology was used, based on the approach developed by Oldenborger (2000) to characterize hydrological conductivity of glacial till. Random sample locations were predetermined and marked on a transparency. The outcrop was viewed through this transparency, held at arm's length from the opposite side of the road, so that the sample locations could be identified and marked (Fig. 2a). This method was found to be effective in producing a random sampling of the outcrop. However, it was not time-efficient, and in some areas it was unsafe due to highway traffic. For these reasons, the primary in situ method was systematic sampling at a fixed interval on a horizontal or vertical bedrock face, perpendicular to the tectonic fabric (if identifiable). The sampling interval varied between 0.1 and 1.0 m, and was selected based on outcrop-scale lithological heterogeneity. Comparison of the two sampling approaches at several locations indicated that statistical parameters of magnetic susceptibility, such as mean and standard deviation, were independent of the choice of sampling methodology (fixed, or pseudo-random). Furthermore, for practical purposes a fixed sampling scheme may be considered as effectively random due to the inherent irregular distribution of lithologies at the outcrop scale; in essence, "nature's randomness compensates for the scientist's regularity" (Middleton, 2000).

Coincident magnetic total-field measurements were acquired at two different locations (stations 200 and 250) to determine the degree of correlation between the susceptibility profile and magnetic anomalies. As no instrument was available for a base station, diurnal activity, as measured by CANMOS (Canadian Magnetic Observatory System) at the

Table 3. Average physical properties of major lithological units in the study area. Lithological subdivisions (*after* Ontario Geological Survey, 1991; Lumbers and Vertolli, 2000) were chosen for the purpose of magnetic-susceptibility classifications.

Lithology	Average in situ (field) magnetic susceptibility (SI)	Average lab magnetic susceptibility (SI)	Average Lab Density (Mg/m^3)	Lithological description
Paleozoic rock	1.71×10^{-6}	1.05×10^{-6}	2.839	Bobcaygeon Formation—Bioclastic limestone, nodular limestone
Metasediments and metavolcanic rocks	7.87×10^{-5}	2.72×10^{-3}	2.720	Mafic and felsic metavolcanic rocks potassium rich to poor, feldspathic gneiss derived from ash flows and tuff, rhyolite and micaceous sandy metasedimentary rocks derived form greywacke-siltstone
Marble	1.00×10^{-6}	5.15×10^{-6}	2.847	Skarn-developed marble with calcareous mixtures of diopside, amphibole, epidote, garnet, K-feldspar, calcite, and quartz
Mafic gneiss	3.41×10^{-3}	1.25×10^{-2}	2.914	Strongly foliated, amphibolite rich (potentially metasedimentary)
Felsic gneiss	1.08×10^{-3}	5.09×10^{-3}	2.787	Diorite, granodiorite, veins of coarse-grained quartzofeldspathic material, to marginally peraluminous alaskite, formed by the assimilation and reaction with marble
Mafic massive rocks	1.69×10^{-3}	2.78×10^{-3}	2.884	Gneissic tonalite, with augen structures and metamorphic fabric
Felsic massive rocks	6.06×10^{-4}	2.86×10^{-3}	2.716	Felsic intrusive rocks with some metamorphic fabric, relict igneous textures, monzogranite, and quartz syenite

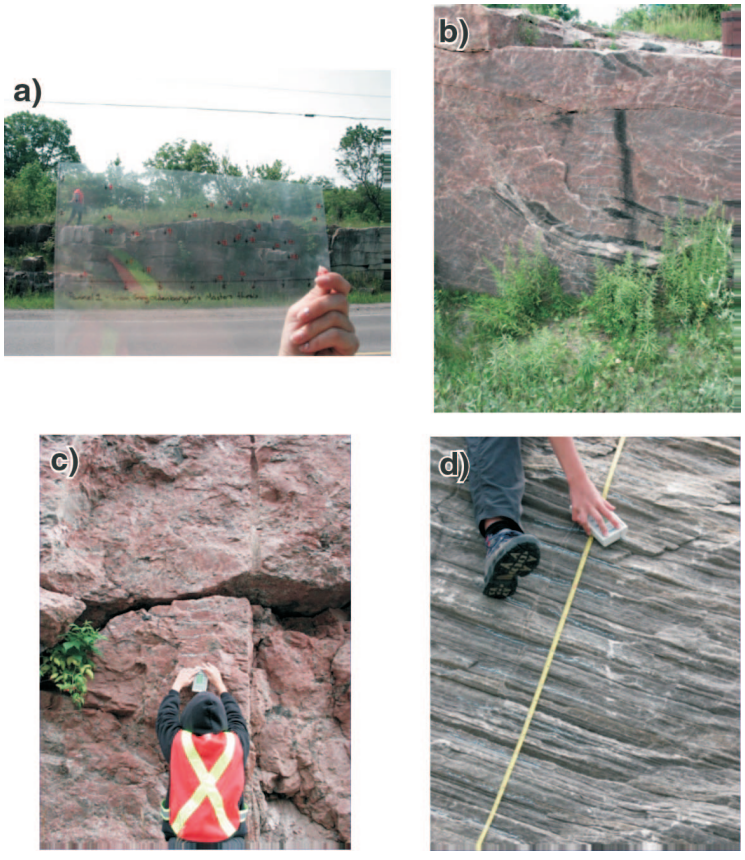

Figure 2.

Photographs of typical sampling locations: ***a)*** *station #200, pseudo-random sampling;* ***b)*** *station #270, sampling interval 10 cm;* ***c)*** *station #275, sampling interval 10 cm;* ***d)*** *station #310, sampling interval 10 cm.*

Ottawa Geomagnetic Observatory at the time of data acquisition, was used to make drift corrections. Due to the relatively large distance (~ 250 km) between the base station and the field area, the diurnal trend was verified by taking a series of measurements at one location for a one-hour time interval. Over one hour, an approximately linear 13 ± 1 nT increase in the magnetic field was observed at both locations; however, the local measurements were affected by short-period fluctuations of up to 4 nT, that were not accounted for in the diurnal correction. Thus, we estimate the uncertainty in our total-field measurement to be ± 4 nT.

At outcrops where a bimodal lithology or significant compositional variations were apparent, care was taken to collect several magnetic-susceptibility profiles to ensure representative coverage of the exposed lithologies. Where the lithology changed within a profile, the data were collected as one profile, with the transition noted. GPS positions and lithological descriptions were recorded at each profile. In cases where two distinct lithologies were located more than 20 m away from each other at a single outcrop, two GPS readings were made and the observations were recorded using two separate station numbers.

Non-oriented, unweathered hand samples were collected in the field for laboratory measurement of their magnetic properties and density. The samples were labelled in the field and entered into a database, together with the in situ magnetic-susceptibility measurement and GPS location. Laboratory and field measurements are summarized in Table 4. The complete set of field and laboratory measurements can be found in O'Dowd (2004) and is also available online at http://www.es.uwo.ca/deaton/cmbbz-mag-database.html

FIELD RESULTS

Correlation of magnetic susceptibility with magnetic anomalies

Figure 3a displays the sampling locations superimposed on a total-field aeromagnetic-anomaly map. Magnetic profiles AB and CD were taken across the strike of the main magnetic anomalies. In Fig. 3b, the extracted magnetic profiles are plotted along with laboratory magnetic-susceptibility measurements (*see* below). A reasonable spatial correlation is evident between high values of K (magnetic susceptibility) and positive magnetic anomalies, particularly for anomalies 3 and 4. Mismatch in location of susceptibility and anomaly peaks may be due to the sparse nature of the susceptibility sampling and the fact that the magnetic data have not been reduced to the pole.

At the outcrop scale, the correlation between magnetic susceptibility and magnetic-anomaly field measured on the ground is less clear. Figure 4 compares two magnetic total-field profiles with their corresponding field magnetic-susceptibility measurements. At station 200, massive to poorly lineated welded tuff of rhyolitic composition is exposed. Magnetic susceptibility readings were made on both the horizontal and vertical faces, with coincident magnetic total-field measurements on the horizontal face. Magnetic total-field readings vary between 54 300 and 54 950 nT, far in excess of the diurnal variations and uncertainties in the instrument readings. The dominant wavelength of the magnetic profile is on the order of 1 m, implying a shallow source. The magnetic susceptibility at this outcrop is generally intermediate to low, with the majority of values being $\leq 2 \times 10^{-4}$ SI. There is no obvious correlation between the magnetic profile and the magnetic-susceptibility readings for this station. It is worth noting that the vertical magnetic susceptibilities have consistently higher values than the measurements made on the horizontal susceptibilities. This may be indicative of magnetic-susceptibility anisotropy as a result of heating of the rock due to metamorphism, or alignment of ferromagnetic minerals during emplacement (Henry et al., 2003).

For the second station (250, Fig. 4b), readings were collected along a 1m profile on the upper surface of the outcrop. This outcrop is a felsic gneiss and has higher magnetic-susceptibility values than the previous example. Here the total-field variation is greater, with the values between 55 000 and 57 500 nT, while magnetic susceptibility values display a broader range between 1.0×10^{-5} and 1.2×10^{-2} SI. The very low magnetic susceptibility readings correspond to pegmatitic dykes of K-feldspar and quartz, while the high regions correspond to more mafic bands within the gneiss. Three positive magnetic anomalies are evident with a dominant wavelength on the order of 1 to 2 m indicating a shallow, local source. These correlate approximately with three zones of elevated magnetic susceptibility.

Magnetic susceptibility versus lithology

Average magnetic-susceptibility measurements are grouped according to lithology in Table 3; Figure 5 shows a box and whisker plot of the field observations. Rock identification and descriptions were based on 1:50 000 Precambrian geology maps of the region (Ontario Geological Survey, 1991; Lumbers and Vertolli, 2000). Lithological units were classified on the basis of general mineralogy and metamorphic intensity. Rocks of sedimentary origin were further subdivided into limestone, marble, and metasedimentary /metavolcanic rock. Siliceous and 'dirty' marbles have been included with the metasedimentary/metavolcanic subdivision, since their magnetic-susceptibility readings are similar. Both massive (igneous) and gneissic rocks were further subdivided into mafic and felsic classifications. Massive assemblages were segregated from gneissic ones to identify any magnetic correlation with metamorphism. Where a bimodal lithology was evident, sample locations were subdivided to better represent the lithological heterogeneity. In situ magnetic-susceptibility measurements are in agreement with previously published data ranges (e.g. Reynolds, 1997). For example, mafic mineral assemblages display the highest magnetic susceptibility (3.14×10^{-3} SI), while sedimentary rocks display the lowest magnetic susceptibility (1.71×10^{-6} SI).

In general, Paleozoic limestone possesses negligible magnetic susceptibility, consistent with the assumptions made in previous studies, e.g. Boyce and Morris (2002). Exceptional

Table 4. Summary of physical-property measurements.

	Latitude	Longitude	Lithology	Wet density		Magnetic susceptibility (SI)			NRM	Königsberger ratio
Sample #	(deg N)	(deg W)		Mg/m^3	Porosity	Field[1]	Field std	Lab	A/m	Qm
110	44.7479	78.6196	2	2.543	0.3%	1.99E-04	1.79E-05	5.83E-05	3.39E+02	3.39E-01
200A	44.5963	78.4513	2	2.654	0.4%	1.04E-04	1.72E-04	3.74E-05	5.74E+02	5.74E-01
200B-1	44.5963	78.4513	2	2.712	0.2%	5.88E-05	1.70E-05	1.58E-05	1.13E+04	1.13E+01
200B-2	44.5963	78.4513	2	2.686	0.3%	1.29E-04	2.95E-05	2.60E-05	5.01E+03	5.01E+00
230B-1	44.602	78.4244	4	2.773	0.1%	1.02E-03	7.97E-04	2.65E-04	2.65E+00	2.65E-03
230B-2	44.602	78.4244	4	2.794	0.0%			9.35E-04	2.95E+00	2.95E-03
230A	44.602	78.4244	7	2.684	0.6%			7.74E-04	2.46E+00	2.46E-03
240	44.61	78.3971	4	2.904	0.0%	4.80E-03	3.37E-03	1.46E-02	2.72E+00	2.72E-03
250-1	44.5817	78.3632	5	2.671	0.2%	5.46E-04	1.78E-02	5.73E-05	3.65E+00	3.65E-03
250-2	44.5817	78.3632	5	2.743	0.2%	2.60E-03	3.31E-03	1.55E-03	3.30E+00	3.30E-03
260-1	44.5697	78.3605	4	2.827	0.0%	5.67E-04	6.15E-02	7.44E-03	1.34E+00	1.34E-03
260-2	44.5697	78.3605	4	2.957	0.0%	1.03E-02	2.77E-02	7.38E-03	2.10E+00	2.10E-03
270A-1	44.5609	78.3435	7	2.652	0.1%	8.88E-04	9.98E-04	1.90E-03	3.25E+00	3.25E-03
270A-2	44.5609	78.3435	7	2.640	0.1%			6.81E-04	3.72E+00	3.72E-03
270B	44.5609	78.3435	7	3.099	0.1%	4.50E-04	6.72E-04	3.63E-04	1.85E+01	1.85E-02
275A-1	44.5664	78.3308	4	3.056	0.1%	3.39E-03	2.81E-03	1.92E-02	8.67E+00	8.67E-03
275A-2	44.5664	78.3308	4	2.922	0.1%			1.55E-02	NA	NA
275B-1	44.5664	78.3308	5	2.965	0.2%	1.10E-04	1.57E-04	1.41E-02	1.12E+01	1.12E-02
275B-2	44.5664	78.3308	5	2.939	0.1%			1.33E-02	9.28E+00	9.28E-03
275C-1	44.5664	78.3308	7	2.566	0.2%			1.13E-03	4.11E+00	4.11E-03
275C-2	44.5664	78.3308	7	2.639	0.1%			1.23E-02	5.94E+00	5.94E-03
280-1	44.5877	78.2632	6	2.732	0.1%	7.07E-04	7.52E-04	1.63E-03	2.19E+00	2.19E-03
280-2	44.5877	78.2632	6	2.765	0.1%	2.55E-05	2.40E-05	1.51E-03	2.08E+00	2.08E-03
295-1	44.5619	78.2145	4	3.016	0.0%	2.40E-03	2.64E-03	2.81E-02	1.01E+01	1.01E-02
295-2	44.5619	78.2145	4	3.037	0.0%			2.48E-02	4.57E+00	4.57E-03
300	44.5734	78.1968	3	2.875	0.5%	1.00E-06	0.00E+00	6.95E-06	1.64E+01	1.64E-02
301A-1	44.5733	78.1973	6	2.884	0.0%	1.23E-03	9.19E-04	3.79E-03	9.03E-01	9.03E-04
301B-1	44.5733	78.1973	6	2.878	0.0%			2.69E-03	2.56E+00	2.56E-03
301B-2	44.5733	78.1973	6	2.884	0.1%			2.83E-03	1.37E+01	1.37E-02
310	44.6046	78.1291	3	2.791	0.1%	5.50E-06	9.24E-06	6.02E-06	2.11E+00	2.11E-03
380A-1	44.7515	78.7237	5	2.755	0.0%	9.76E-04	4.29E-04	4.34E-03	8.13E+00	8.13E-03
380A-2	44.7515	78.7237	5	2.706	0.1%			2.07E-03	5.91E+00	5.91E-03
380C	44.7515	78.7237	6	3.161	0.0%			4.22E-03	8.87E+00	8.87E-03
380B	44.7515	78.7237	7	2.733	0.1%			2.92E-03	2.43E+00	2.43E-03
390-1	44.7477	78.7394	1	2.846	0.1%	1.00E-06	0.00E+00	1.20E-06	3.68E+00	3.68E-03
390-2	44.7477	78.7394	1	2.832	0.1%			9.01E-07	4.93E+00	4.93E-03
400-1	44.7434	78.7764	3	2.834	0.2%	1.00E-06	0.00E+00	5.19E-06	3.94E+01	3.94E-02

[1] Mean value of field measurements. Note that at some locations, more than one lab sample was collected, but field data are reported only once. For complete set of field observations, see http://www.es.uwo.ca/deaton/cmbbz-mag-database.html.

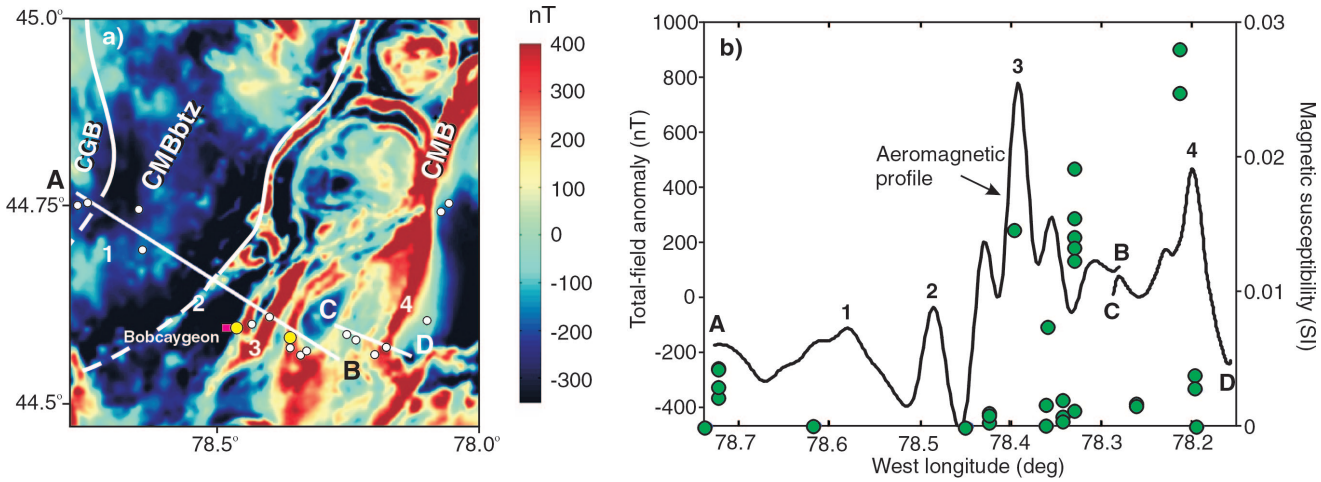

Figure 3. a) *Total-field aeromagnetic anomaly map for the area outlined by the box in Fig. 1. Sampling locations are indicated by circles. Ground magnetometer profiling locations are indicated by larger yellow circles.* ***b)*** *Magnetic profiles A-B and C-D extracted from the total-field map on left, showing laboratory magnetic-susceptibility measurements. CGB – Central Gneiss Belt, CMB – Central Metasedimentary Belt, CMBbtz – Central Metasedimentary Belt boundary tectonic zone.*

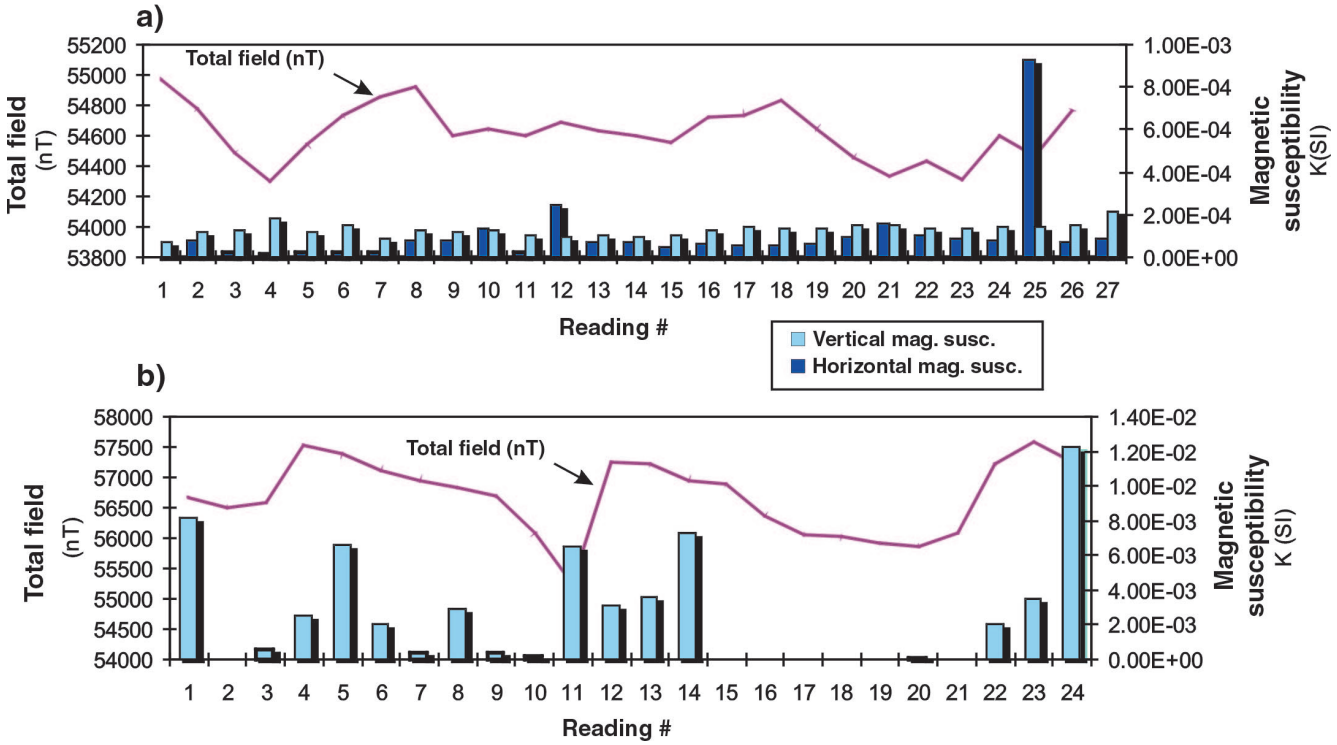

Figure 4. *Comparison of magnetic-susceptibility readings with coincident ground total-field profiles at* ***a)*** *station 200, and* ***b)*** *station 250. Profile locations are indicated in Fig. 3a. Width of the line shows uncertainty in magnetic-profile measurements. Sampling interval is 1 m. Vertical and horizontal susceptibility refer to measurements on horizontal and vertical rock faces, respectively.*

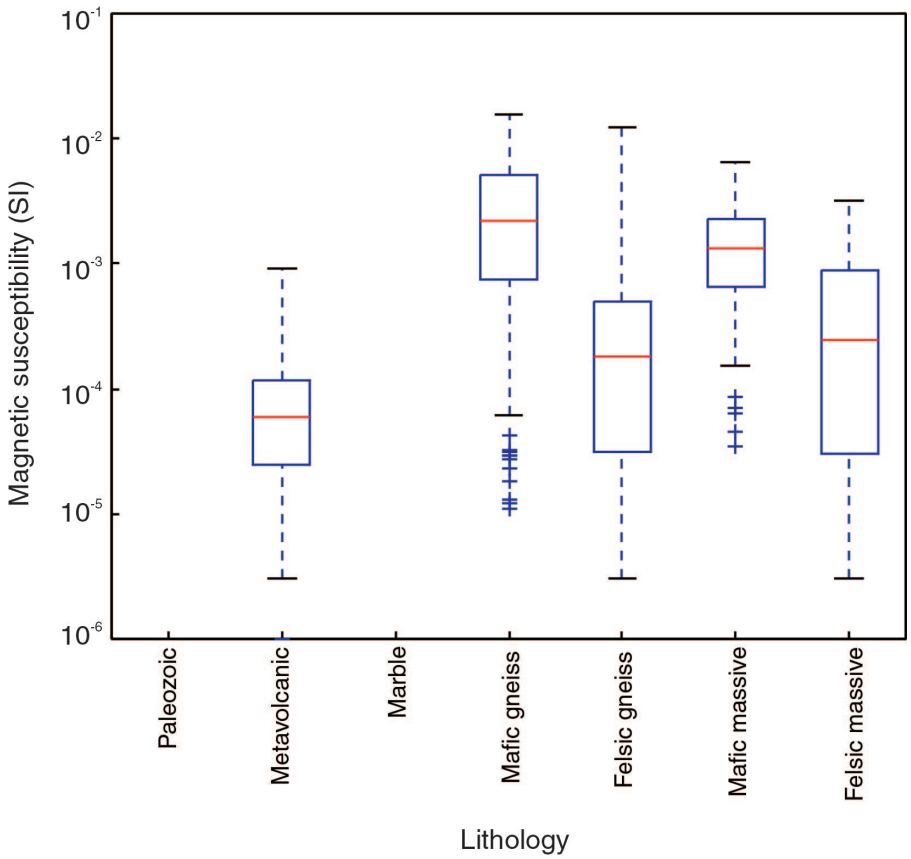

Figure 5.

Box-and-whisker plot of field observations of magnetic susceptibility, grouped by lithology. Red line indicates logarithmic mean, box outlines 25th to 75th logarithmic percentiles, crosses identify outliers.

cases of enhanced susceptibility of Paleozoic limestone were observed at the Precambrian unconformity. In such cases, the rocks are extremely weathered and have a rusty appearance.

LABORATORY METHODS

Sample preparation

Rock samples collected in the field were cut into slabs and then cored using a 2.54 cm stainless steel drill bit. These cores, which were cut approximately perpendicular to any visible fabric, were then cut into 2.54 cm 'pucks' using two steel tile saws. Some samples fell apart prior to measurement due to their fissile nature and are therefore not included in the results given here. The pucks were then ground on the flat surfaces using 220 µm silicon carbide grit to remove any remanent magnetic contamination from the saw blades. The drill bit is assumed to add no contamination to the samples, since stainless steel is non-magnetic.

Density Measurements

Density calculations were carried out by measuring the volume and mass of each puck. Callipers were used to measure the height and width of each cylindrical puck, from which the volume was calculated. Samples were measured for dry mass then were soaked for 4 days in de-ionized water (density =1.000 Mg/m^3) and remeasured for saturated mass. This approach resulted in measurement uncertainties of ≤ 0.0007 Mg/m^3.

Magnetic Susceptibility and Königsberger ratio

Magnetic susceptibilities were measured using a SI2B magnetic susceptibility and anisotropy meter. The specifications for laboratory instruments are given in Table 2. Each puck was measured twice with two air readings, that were averaged to correct for any instrument drift. The magnetic susceptibility was calculated from the ratio of the inductances and corrected for drift by performing three coil-inductances measurements. The first and third measurements were made with the sample removed and the second with the sample inside the coil. Measurements were made in units of cgs mass susceptibility and converted to standard SI (volume) susceptibility by multiplying the reading by 4π and dividing by the density of the sample. The total natural remanent magnetization (NRM) of each sample was measured using a Digital Spinner Magnetometer (DMS-1).

LABORATORY RESULTS

Density

Laboratory measurements of density are listed in Table 4. Figure 6a shows the regional Bouguer gravity map, with profile AB extracted along the main sampling corridor.

In Fig. 6b, the gravity profile is plotted with laboratory sample densities. Although sampling distribution is sparse, there is good correlation between the densities and the gravity profile. In particular, a prominent gravity low associated with the Central Metasedimentary Belt boundary tectonic zone correlates with micaceous metavolcanic rocks with very low density. Figure 7 shows a box-and-whisker plot of the wet density. Mafic lithologies have the highest average density (~2.91 Mg/m^3), while the metavolcanic and metasedimentary samples have the lowest density (~2.71 Mg/m^3). Marble and Paleozoic limestone have intermediate densities (~2.84 Mg/m^3).

Percentage porosity (*Pp*) was calculated from the wet and dry densities as follows:

$$Pp = (M_s - M_d/V)\text{x}100 \quad (1)$$

where M_s is the saturated mass, M_d is the dry mass and V is the sample volume. In every case, the porosity was found to be less than 1% (Table 4).

Magnetic susceptibility

Three distinct groups of magnetic susceptibility data are evident from the laboratory measurements (Figure 8, Table 3). Mafic gneiss lithologies possess the highest magnetic susceptibility, with a mean magnetic susceptibility of 1.25x10^{-2} SI. Marble, and Paleozoic limestone have a relatively low mean magnetic susceptibility in the range of 1.05x10^{-6} to 5.15x10^{-6} SI. The third cluster of data corresponds with metasediments, felsic gneiss, felsic massive and mafic massive lithologies, where the mean magnetic susceptibility ranged from 2.72x10^{-3} to 5.09x10^{-3} SI.

Königsberger ratio

The Königsberger ratio was calculated using:

$$Q = J_R/J_I, \quad (2)$$

where J_R is the measured NRM, $J_I = K\text{x}H$ is the induced magnetization, K is the magnetic susceptibility (SI) as determined previously, and H is the magnetic-field intensity. Very low Königsberger ratios (Q<0.01) were determined for all but four rock samples, implying that magnetic anomalies in this area are a result of induced magnetization and not remanent magnetization. The four samples that possess higher Q values are associated with extremely low magnetic susceptibility values (Figure 9) and hence make a very small contribution to the observed magnetic anomalies. This result is consistent with the common practice of neglecting NRM for interpreting magnetic anomalies (Hope and Eaton, 2002).

Comparison of laboratory and field magnetic susceptibility

Laboratory magnetic-susceptibility measurements are made under controlled conditions, with the sample placed inside the measuring coil rather than adjacent to the coil. Hence, we regard laboratory measurements to be more reliable than the in situ measurements. Figure 10 compares the laboratory and in situ measurements of the magnetic susceptibility. Laboratory measurements for Paleozoic limestone and marble units are lower field measurements. Such results can be explained by contamination from weathering, leaching of magnetic minerals from soil, and assorted random magnetic minerals that were not present in the unweathered samples measured in the laboratory. In general, high magnetic-susceptibility measurements result from high mafic-mineral content. In this study, the authors found that the absolute

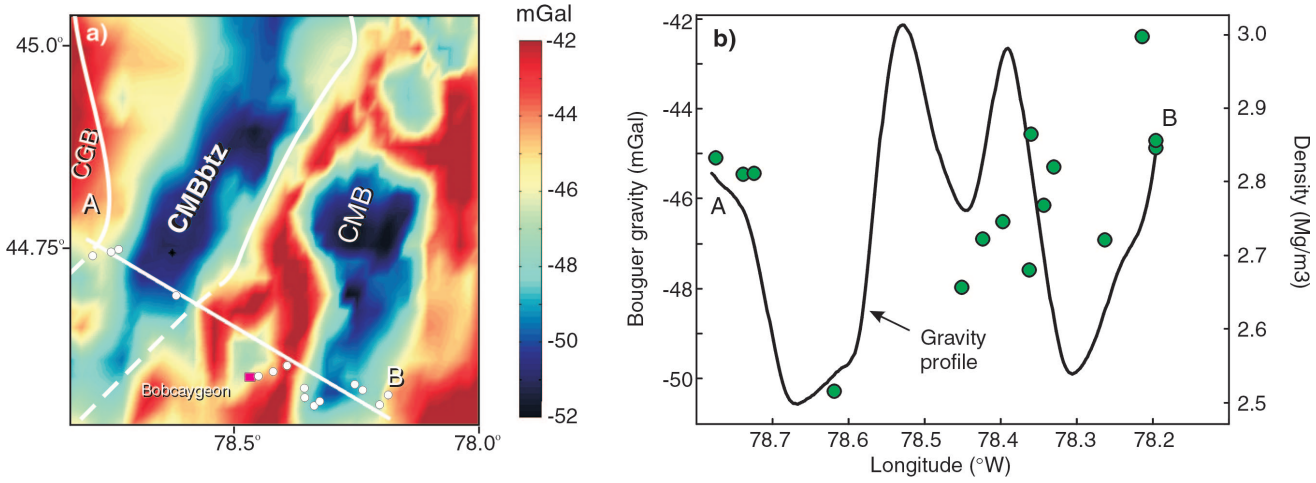

Figure 6. a) *Bouguer anomaly map of the study area. Sampling locations are indicated by circles.* ***b)*** *Gravity profile A-B extracted from the Bouguer gravity map on left, showing laboratory density measurements. CGB – Central Gneiss Belt, CMB – Central Metasedimentary Belt, CMBbtz – Central Metasedimentary Belt boundary tectonic zone.*

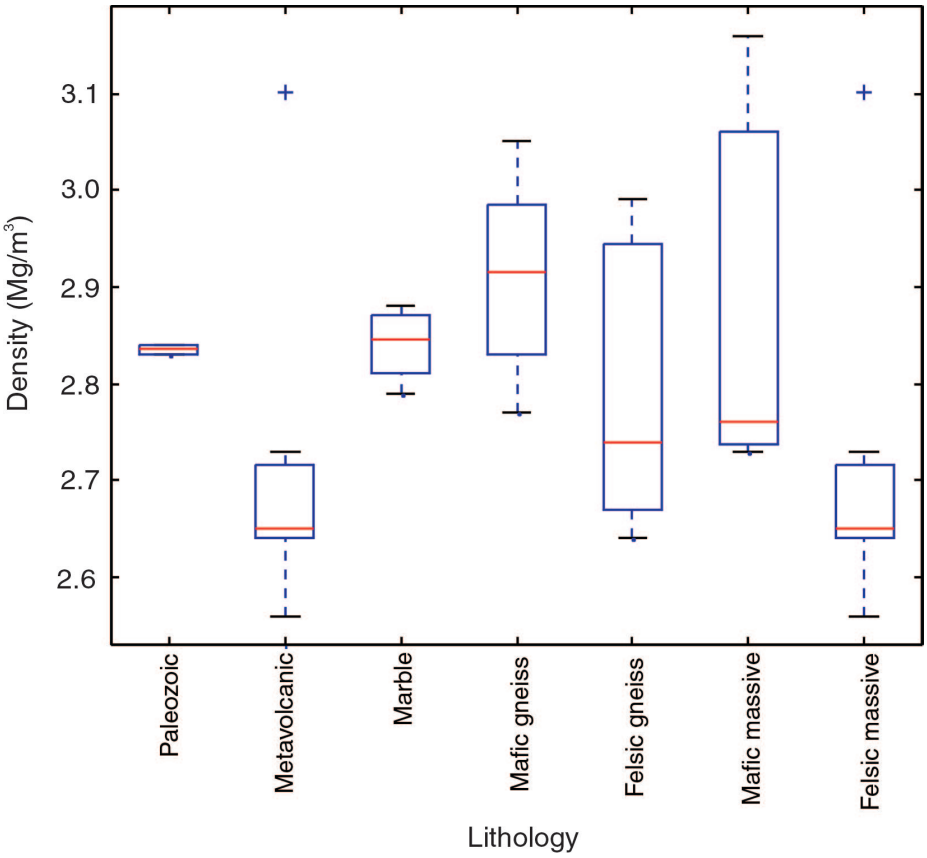

Figure 7.

Box-and-whisker plot of wet density, grouped by lithology. Red line indicates mean, box outlines 25th to 75th percentiles, crosses identify outliers.

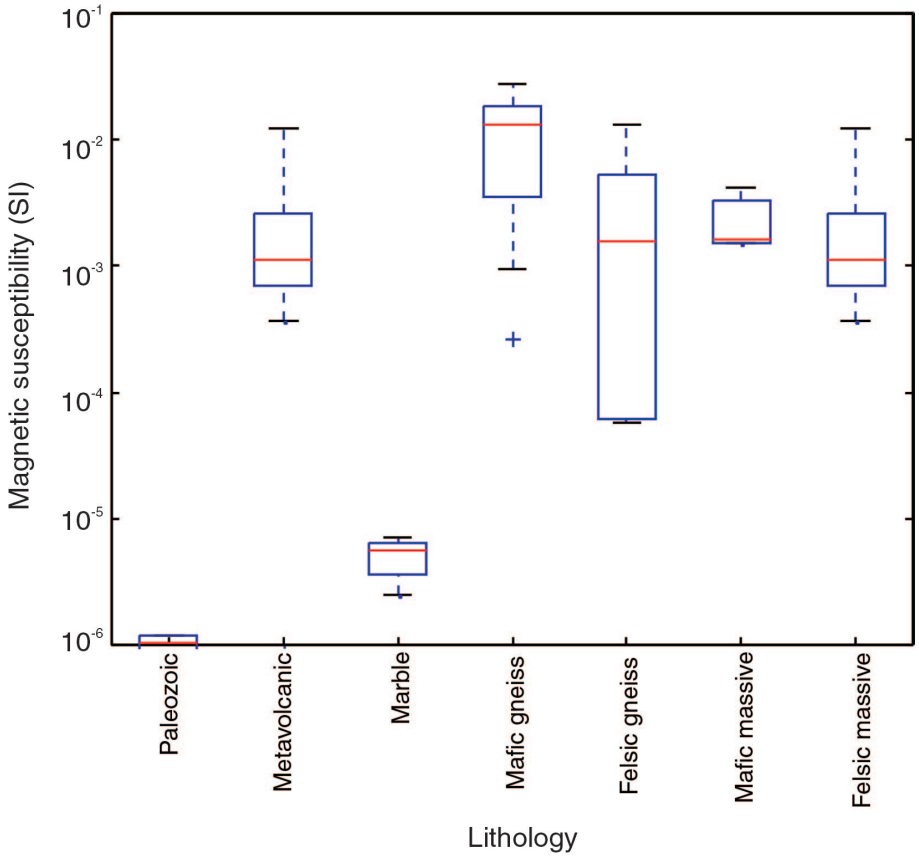

Figure 8.

Box-and-whisker plot of laboratory observations of magnetic susceptibility, grouped by lithology. Red line indicates logarithmic mean, box outlines 25th to 75th logarithmic percentiles, crosses identify outliers.

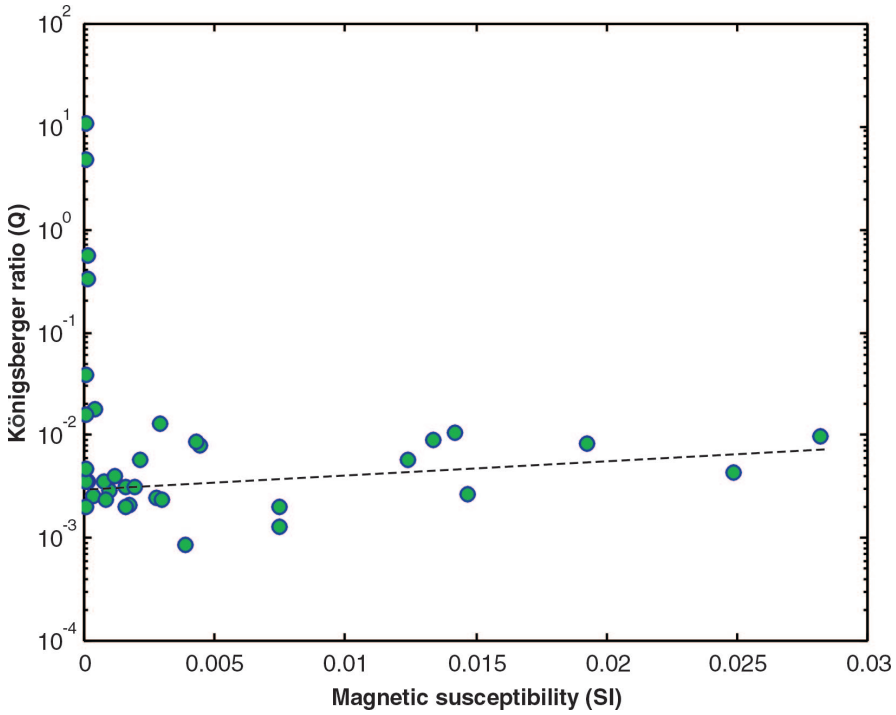

Figure 9.

Königsberger ratio (Q) versus laboratory magnetic susceptibility (K). Almost all samples are characterized by Q < 0.01. There appears to be a weak positive correlation of Q with K, as indicated by the dashed line.

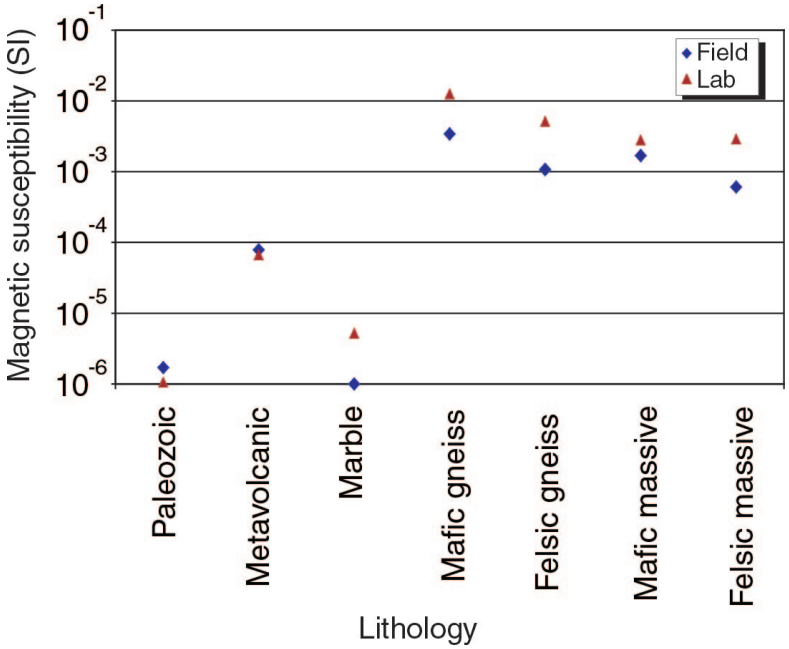

Figure 10.

Comparison of laboratory and field measurements of magnetic susceptibility (K).

deviation between laboratory susceptibility readings and measurements made in situ tended to increase with magnetic susceptibility.

CONCLUSIONS

1. Measured magnetic susceptibilities for rock units near Bobcaygeon, Ontario within the Central Metasedimentary Belt, Central Metasedimentary Belt boundary tectonic zone, and Central Gneiss Belt, follow expected compositional trends. Mafic gneissic lithologies possess the highest mean values of susceptibility (1.25×10^{-2} SI). The units of felsic gneiss, and mafic and felsic massive lithologies possess intermediate susceptibility values of 2.72×10^{-3} to 5.09×10^{-3} SI, with a strong dependence on the distribution of the mafic minerals. Limestone and marble have very low magnetic susceptibility, as expected from of the lack of magnetic minerals present.
2. In situ measurements appear to underestimate the susceptibility of more magnetic rocks, compared to laboratory measurements.

3. On a regional scale, a good correlation is apparent between large values of magnetic susceptibility and positive aeromagnetic anomalies, although at outcrop scale these correlations are not as clear.

4. There is some evidence for anisotropy of magnetic susceptibility, with measurements obtained from a vertical face being consistently lower than measurements made on the adjacent horizontal face.

5. Small observed Königsberger ratios (<0.01) for most samples are consistent with the practice of neglecting remanent magnetization in the interpretations of magnetic anomalies from within the Grenville Province.

6. Density values are generally consistent with expected results. Mafic lithologies have the greatest density (~2.91 Mg/m^3), low-porosity marble, limestone and felsic lithologies posses intermediate densities (~2.84 Mg/m^3), and highly micaceous metasediment/metavolcanic lithologies have lower densities (~2.71 Mg/m^3).

It is hoped that these results will provide useful constraints for future potential-field (gravity and magnetic) modelling and inversion studies in this region.

ACKNOWLEDGMENTS

Gravity and magnetic data were provided by the Geophysical Data Centre, Geological Survey of Canada. We are grateful to Lisa Freidrich for her assistance during field-sample collection, Gord Wood for assistance with sample preparation, and Dr. Currie Palmer for the assistance in magnetic-susceptibility measurements. This manuscript benefited from critical reviews by Mark Pilkington and Pierre Keating.

REFERENCES

Boyce, M., and Morris, W.
2002: Basement-controlled faulting of Paleozoic strata in southern Ontario, Canada: new evidence from geophysical lineament mapping; Tectonophysics, v. 353, p. 151–171.

Easton R.M. and Carter, T.R.
1995: Geology of the Precambrian basement beneath the Paleozoic of southwestern Ontario; *in* Basement Tectonics, (ed.) R.W. Ojakangas, Proceedings of the International Conference on Basement Tectonics, v.10, p. 221–264.

Forsyth, D.A., Milkereit, B. Zelt, C.A., White, D.J., Easton, R.M., and Hutchinson, D.R.
1994: Deep structure beneath Lake Ontario: crustal-scale Grenville Subdivisions; Canadian Journal of Earth Sciences, v. 31, p. 225–270.

Gupta, V.K.
1991: Shaded image of total magnetic field of Ontario, southern sheet; Ontario Geological Survey, Map 2587, scale 1:1000000.

Hanmer, S. and McEachern, S.J.
1992: Kinematical and rheological evolution of a crustal-scale ductile thrust zone, Central Metasedimentary Belt, Grenville Orogen; Canadian Journal of Earth Sciences, v. 29, p. 1779—1790.

Henry, B., Jordanova, D., Jordanova, N., Souque, C., and Robion, P.
2003 : Anisotropy of magnetic susceptibility of heated rocks; Tectonophysics, v. 366, p. 241–258

Hope, J. and Eaton, D.
2002: Crustal structure beneath the Western Canada Sedimentary Basin: constraints from gravity and magnetic modelling; Canadian Journal of Earth Sciences, v. 39, p. 219–312

Lidiak, E.G. and Hinze, W.J.
1993: Grenville Province in the subsurface of eastern United States; *in* Precambrian: Conterminous United States, (ed.) J.C. Reed, Jr., The Geology of North America, Volume C-2, p. 535–365.

Lumbers, S.B. and Vertolli, V.M.
2000: Precambrian Geology, Burleigh Falls Area; Ontario Geological Survey, Map P.3404, scale 1:50 000.

Middleton, G.
2000: Data analysis in the earth sciences using MATLAB®; (ed) Lynck, P., Prentice-Hall, New York, New York, p. 10–18.

Milkereit, B., Forsyth, D.A., Green, A.G., Davidson, A., Hanmer, S., Hutchinson, D., Hinze, W.J., and Mereu, R.F.
1992: Seismic images of a Grenvillian terrane boundary; Geology, v. 20, p. 1027–1030.

O'Dowd, C.R., Eaton, D., Forsyth, D. and Asmis, H.W.
2004: Structural fabric of the Central Metasedimentary Belt of southern Ontario, Canada, from deep seismic profiling; Tectonophysics, v. 388, p. 145–159.

Oldenborger, G.
2000: Characterizing the spatial distribution of hydraulic conductivity: application of ground-penetrating radar and space-local spectral techniques; M.Sc. thesis, Faculty of Earth Science, University of Western Ontario, London, Ontario, 128 p.

Ontario Geological Survey
1991: Bedrock Geology of Ontario, Southern Sheet; Ontario Geological Survey, Map 2544, Scale 1:1 000 000.

Ouassa, K. and Forsyth, D.
2002: Interpretation of seismic and potential field data from western New York State and Lake Ontario; Tectonophysics, v. 353, 115–149.

Reynolds, J.M.
1997: An introduction to applied and environmental geophysics; John Wiley and Sons, 806 p.

Rivers, T.
1997: Lithotectonic elements of the Grenville Province: review and tectonic implications; Precambrian Research, v. 86, p. 117–154.